*Studia Geotechnica et Mechanica, Vol. XXX, No. 1–2, 2008*

# DEM NUMERICAL ANALYSIS OF LOAD TRANSFERS IN GRANULAR SOIL LAYER

BASTIEN CHEVALIER, GAËL COMBE, PASCAL VILLARD

Laboratoire 3S-R: Sols, Solides Structures et Risques,
BP 53-38041 Grenoble cedex 9 France, e.mail: bastien.chevalier@ujf-grenoble.fr

**Abstract:** Load transfers and other arching effects are mechanisms frequently met in civil engineering, especially in areas subject to karstic subsidence or in geotechnical earth structures such as piled embankments. The study proposed focuses on the numerical discrete analysis of granular material response submitted to specific boundary conditions leading to load transfer (embankment built over a trench or over a network of piles). The influence of several parameters has been studied: granular layer thickness, friction behaviour and particle shapes. Various load transfer mechanisms are observed, depending on the boundaries and also on the granular layer properties. The comparison between three-dimensional Discrete Element Modelling and analytical calculation methods leads to a various agreement, depending on the case treated.

## 1. INTRODUCTION

Load transfer and other arching effects are commonly met in geotechnical earth structures such as piled embankments or embankments submitted to karstic subsidence. Actually the behaviour of such a phenomenon is not well established and a lot of answers to the influence of major parameters as structure geometry or mechanical properties of the soil need to be found. There is a great variety of analytical or empirical approaches that have been developed: some consider particular shear planes for load transfer [1], others take into account the formation of idealized arches of different shapes [2]–[4]. Due to the specific assumptions made, the predicted results of the actual analytical methods vary greatly from one to another.

In order to better understand these phenomena and to highlight the arching effect, a numerical parametric study based on a numerical discrete element approach was carried out. This study focuses on the numerical response of a particles assembly submitted to specific boundary conditions leading to load transfer over a trench or over a network o piles. The 3D Distinct Element Method used allows reproducing the behaviours of granular materials (particles reorganization, collapse, dilatancy …).

## 2. NUMERICAL MODEL AND PROCEDURE

### 2.1. THE DISTINCT ELEMENT METHOD

A granular material being modelled is composed of deformable particles (molecular dynamics) that interact with each other through contact points. At each contact

point, normal and tangential contact forces are governed by linear contact laws [5]. The normal contact force between two particles *i* and *j* can be written:

$$f_n^{ij} = K_n h^{ij}, \tag{1}$$

where $K_n$ represents the normal stiffness of the contact and $h^{ij}$ the overlap of the two particles *i* and *j*. The tangential contact force $f_t^{ij}$ is linked with the incremental relative displacement $\varepsilon$ of the particles *i* and *j* by a tangential stiffness $K_t$:

$$\frac{df_t^{ij}}{d\varepsilon} = K_t \tag{2}$$

with the condition $\| f_t^{ij} \| \leq \mu f_n^{ij}$ where $\mu$ is the contact friction coefficient.

The discrete element code used is a three-dimensional software (SDEC [6]).

### 2.2. GEOMETRY OF THE NUMERICAL MODEL

A granular layer is laid at fixed porosity with the REDF process [7] (radius expansion with decreasing friction) in a box delimited at the bottom by a horizontal frictional wall referred to as plate and on the sides by frictionless rigid walls. The load transfer mechanisms are obtained under gravity by moving down by small increments of displacement the middle part of the horizontal plate. The fixed parts of the bottom plate called supports have a friction coefficient $\mu$.

Two different applications have been studied. The first pattern (figure 1) provides the example of a granular layer built over a trench. The second pattern (figure 2) deals with the numerical modelling of an embankment built on a soft soil reinforced with inclusions.

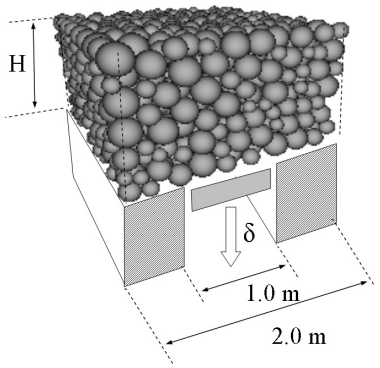


Fig. 1. Granular layer over a trap-door

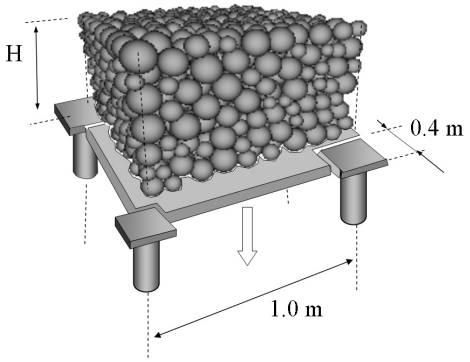


Fig. 2. Granular layer over a network of piles

## 2.3. PHYSICAL PROPERTIES OF THE GRANULAR MATERIALS

The macroscopic behaviour of a particles' assembly depends on the geometry, the grading, the initial porosity and the micromechanical parameter used. In order to determine the influence of particle shape and friction parameters, three dense and cohesionless granular materials called $M_i$, $i$ = 1, 2, 3, were taken into account for the numerical simulations. Material $M_1$ is only composed of the spheres uniformly distributed in size between minimal and maximal diameters $d_{\min}$ and $d_{\max} = 4d_{\min}$. The number of particles per $m^3$ is constant and equal to 8000.

Materials $M_2$ and $M_3$ are composed of the clusters made up of two jointed particles of the same diameter. The distance between the centres of two jointed spheres is 95% of their diameter. The particle sizes are also uniformly distributed between $d_{\min}$ and $d_{\max}$.

Table

Characteristics of the granular assemblies

| Characteristics | $M_1$ | $M_2$ | $M_3$ |
|---|---|---|---|
| Shape | circular | cluster | cluster |
| Porosity | 0.355 | 0.355 | 0.355 |
| Grain density [kg.m$^{-3}$] | 2650 | 2650 | 2650 |
| Apparent density [kg.m$^{-3}$] | 1600 | 1600 | 1600 |
| $\kappa$ [–] | 800 | 800 | 800 |
| $k_s/k_n$ | 0.75 | 0.75 | 0.75 |
| $\mu$ | 0.577 | 0.176 | 0.364 |
| Young modulus [MPa] | 9.2 | 12.9 | 11.2 |
| Poisson coefficient | 0.12 | 0.11 | 0.11 |
| Peak friction angle $\varphi_{\text{peak}}$ | 27° | 27° | 39° |
| Residual friction angle $\varphi_r$ | 22.3° | 24.7° | 29.5° |

For a set of micromechanical parameters (the table), the mechanical characteristics of materials $M_1$ to $M_3$ have been determined by a numerical modelling of a triaxial test under an initial low isotropic pressure of 16 kPa (figure 3). The friction microparameter $\mu$ of contact for material $M_2$ (the table) is chosen in order to obtain an equivalent macroscopic shear strength rather than that obtained with the granular assembly of material $M_1$. This equivalence of shear strength is based on the value the internal friction angle $\varphi_{\text{peak}}$. So the value of the friction parameter of contact of material $M_2$ is low. Frictional parameter of material $M_3$ (similar to that of material $M_2$) is increased in order to test the influence of the internal friction angle on the arching effect. Each $M_i$ has the same stiffness level $\kappa$ [8]:

$$\kappa = \frac{\langle K_n \rangle}{\langle d \rangle P} = 800\,, \tag{3}$$

where $\langle K_n \rangle$ is the average normal contact stiffness, $\langle d \rangle$ stands for the average diameter of the particles and $P$ is the isotropic pressure level. $1/\kappa$ represents the mean overlap of the granular material.

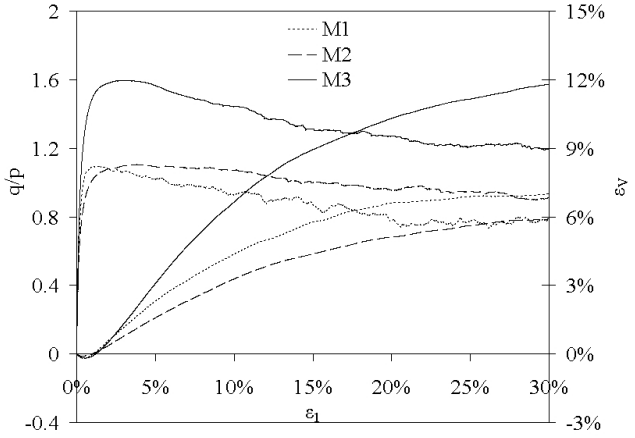


Fig. 3. Numerical macroscopic behaviour of particles' assembly for a triaxial test under an initial isotropic pressure of 16 kPa

## 3. APPLICATION TO THE TRAP-DOOR PROBLEM

This part of the study deals with the theoretical case described by TERZAGHI [1] and illustrated in figure 1, which defines the stress $s$ applied to a mobile plate

$$s = \frac{L\gamma}{2K_a \tan\varphi}(1 - e^{-K_a \tan\varphi \, 2H/L}), \tag{4}$$

where: $L$ is the width of the trap-door, $K_a = (1 - \sin\varphi_{\text{peak}})/(1 + \sin\varphi_{\text{peak}})$ is the active earth pressure coefficient, $H$ is the granular layer thickness, $\varphi$ is the internal friction angle and $\gamma$ is the apparent density of the granular layer.

### 3.1. INFLUENCE OF THE SHAPE OF THE PARTICLES BY THE COMPARISON OF $M_1$ AND $M_2$

The modelled granular materials $M_1$ and $M_2$ are composed, respectively, of spherical particles and clusters. The comparison of their behaviour for the trap-door configuration for several heights of the granular assembly will allow appreciating the effect of the shape of the particles.

The variation of the force $F$ acting on the trap-door versus the vertical displacement of the plate $\delta$ is given in figure 4.

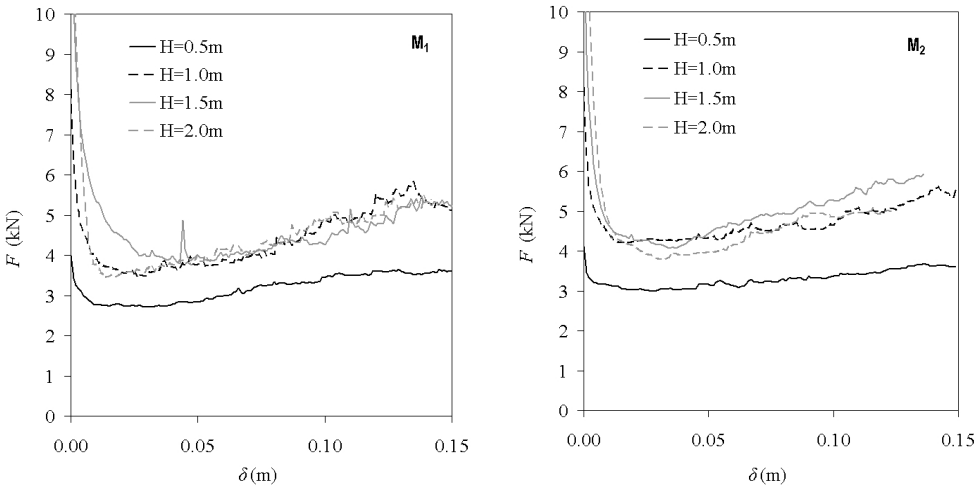


Fig. 4. $F$ versus $\delta$ in the trap-door application for $M_1$ (left) and $M_2$ (right)

In all the cases, $F$ first decreases quickly when $\delta$ increases until a minimum is reached. Then, $F$ increases with $\delta$ and reaches a final value ($\delta \geq 0.12$ m) In the case $M_1$, the minimal force $F_{min}$ acting on the trap-door is slightly more important than in the case $M_2$. The difference between the two behaviours obtained is not major. The load transfer intensity essentially depends on the macroscopic shear strength of the granular material. A critical layer thickness $h_c$ can be found above which the minimal effort applied to the trap-door does not vary anymore: $0.5 \leq h_c \leq 1.0$ (m) for both materials. For $h \geq h_c$, an increase in the layer thickness is equivalent to the application of a uniform load.

The efficacy of a granular layer built over a subsiding trench is defined by TERZAGHI [1]:

$$E_T = 1 - \frac{W_B}{W}, \tag{5}$$

where $W_B$ is the resulting vertical force acting on the mobile plate, and $W$ is the weight of the granular layer located just over the trench. The efficacy of the granular layer, calculated from the value of $F$ corresponding to the final state ($\delta = 0.12$ m), is given in figure 5 for different values of $H$. The efficacies calculated from [1] are also represented.

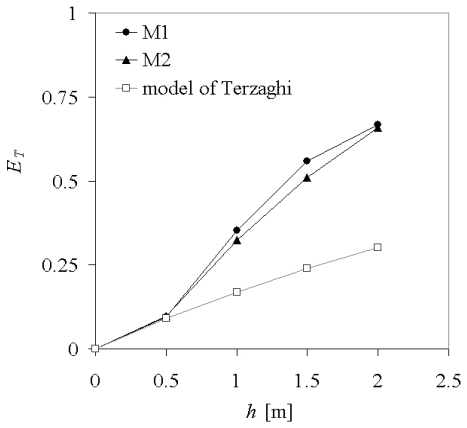


Fig. 5. Comparison of the numerical results ($M_1$ and $M_2$, $\delta = 0.12$ m) and the prediction of TERZAGHI [1]

The comparison of the numerical results with the model of TERZAGHI [1] (figure 5) is satisfying for low values of $H$ but is no longer valid for higher $H$. Figures 6 and 7 show a graphic representation of the displacement field of particles located in a cross

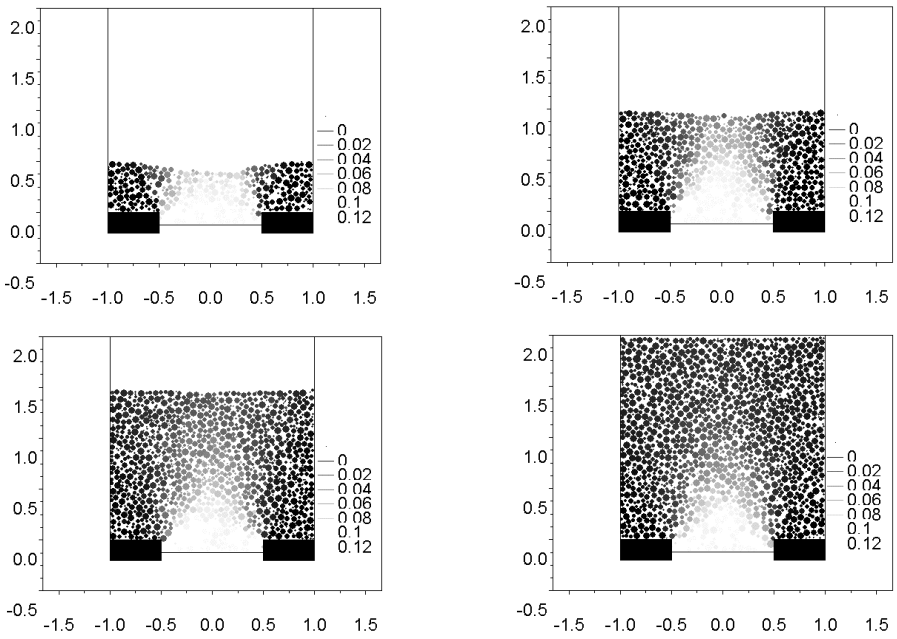


Fig. 6. Displacement field of the particles in a cross section of the granular layer ($M_1$) for $\delta = 0.12$ m and for different layer thicknesses (gray scale unit [m])

section of the granular layer (for $\delta = 0.12$ m) for $M_1$ and $M_2$. For $H \leq 1.0$ m, the vertical column of granular material located just above the trap-door moves vertically, while the part of the layer located above the lateral supports stays fixed. This observation, in accordance with the Terzaghi assumptions, explains the good agreement of analytical and numerical results for $H < 1.0$ m. On the contrary, for $H > 1.0$ m, the column located above the trap-door moves downward only in its lower part.

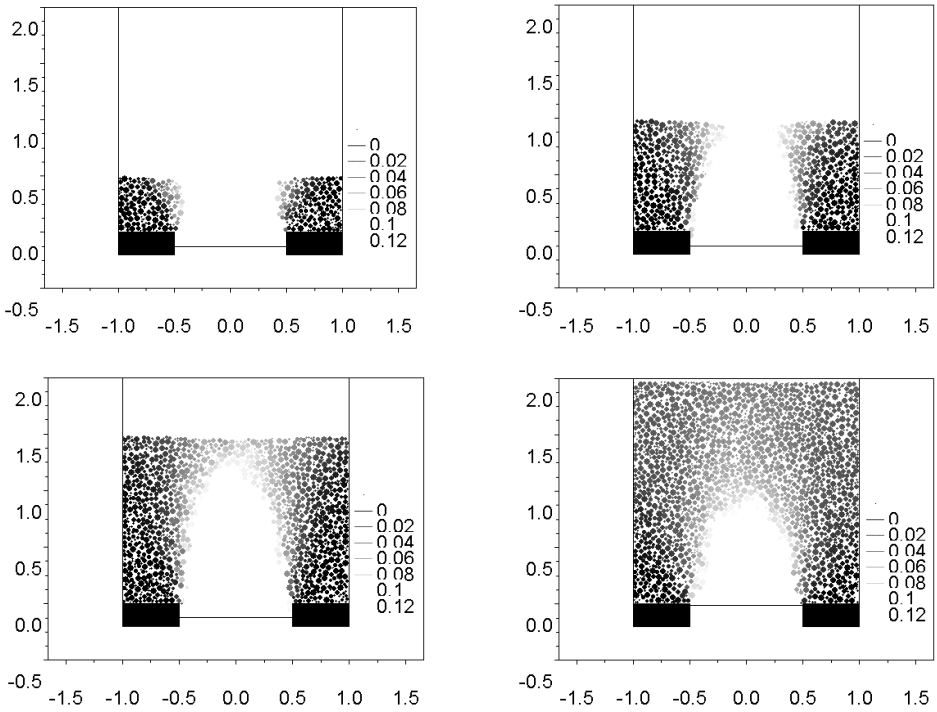


Fig. 7. Displacement field of the particles in a cross section of the granular layer ($M_2$) for $\delta = 0.12$ m and for different layer thicknesses (gray scale unit [m])

The settlements observed on the top of the layer constantly decrease as the layer thickness increases (figure 8). It can be deduced from this result that no real arch is formed in the case of $M_1$ and $M_2$. Indeed, should an arch be formed in the granular material, the increase of the layer thickness might not influence the settlements measured on top of the layer.

In order to analyse the numerical results, two particle families can be defined:

- the particles distributed along vertical axis above support, called ($\Delta$),
- the particles distributed along vertical axis above mobile plate, called ($\Delta'$).

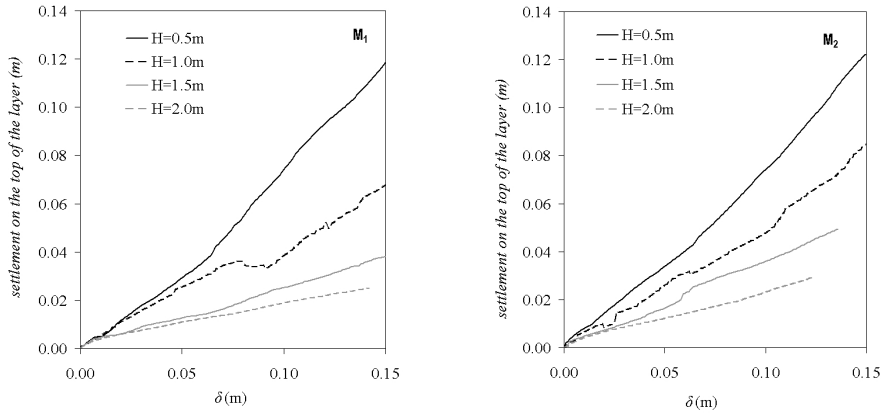


Fig. 8. Maximal value of the settlement measured on the surface of the granular layer for $M_1$ (left) and $M_2$ (right)

For these two particle families, the $Z$-axis positions versus the particle displacement have been represented for $\delta = 0.12$ m and $H = 2.0$ m (figure 9). Two distinct zones can be highlighted on this graph. In the lowest part of the layer ($H < 1.0$ m), the relative slipping of the material above the mobile plate with the material above supports is very important. In the upper part of the layer, this relative slipping is strongly reduced.

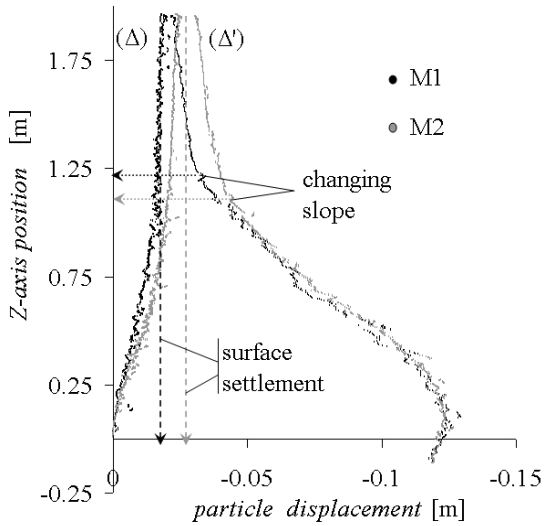


Fig. 9. Vertical displacements along (Δ) (left curves) and (Δ′) (right curves) for $M_1$ and $M_2$ ($\delta = 0.12$ m)

In this case, the influence of the particle shape is not really significant for the efficacy of the granular layer. However, the displacements are more important with $M_2$ than with $M_1$, probably due to the very low value of the microscopic friction coefficient $\mu$ in the case of $M_2$.

### 3.2. INFLUENCE OF THE PEAK FRICTION ANGLE BY COMPARISON OF $M_2$ AND $M_3$

The materials $M_2$ and $M_3$ subjected to modelling are compared (the table). The only varying parameter is $\varphi_{peak}$ which depends exclusively on $\mu$; in this case: $\varphi_{peak}$ ($M_2$) = 27° and $\varphi_{peak}$ ($M_3$) = 39°. The variation of $F$ with $\delta$ is given in figure 10 ($M_3$).

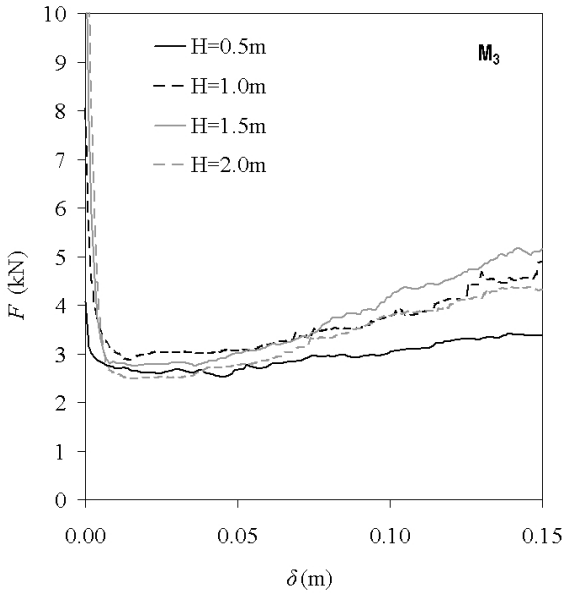


Fig. 10. $F$ versus $\delta$ in the trap-door problem for $M_3$

The same phases can be underlined in order to describe the behaviour of the layer: a quick decrease, then a minimum and finally a progressive increase of $F$ with $\delta$. The critical height $H_c$ is lower for $M_3$ than for $M_2$; $H_c \leq 0.5$ m.

The load transfer increases with the shear strength (i.e., $\varphi_{peak}$). As shown in figure 11, the divergence between the numerical results and predicted efficacies obtained from the theory of Terzaghi is confirmed with $M_3$, but the divergence of the lowest values of $H$ is also observed.

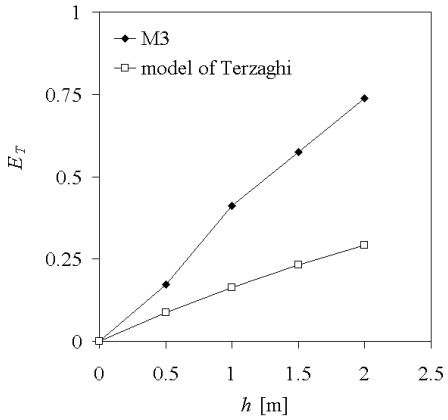


Fig. 11. Comparison of the numerical results $M_3$ with the prediction of TERZAGHI [1]

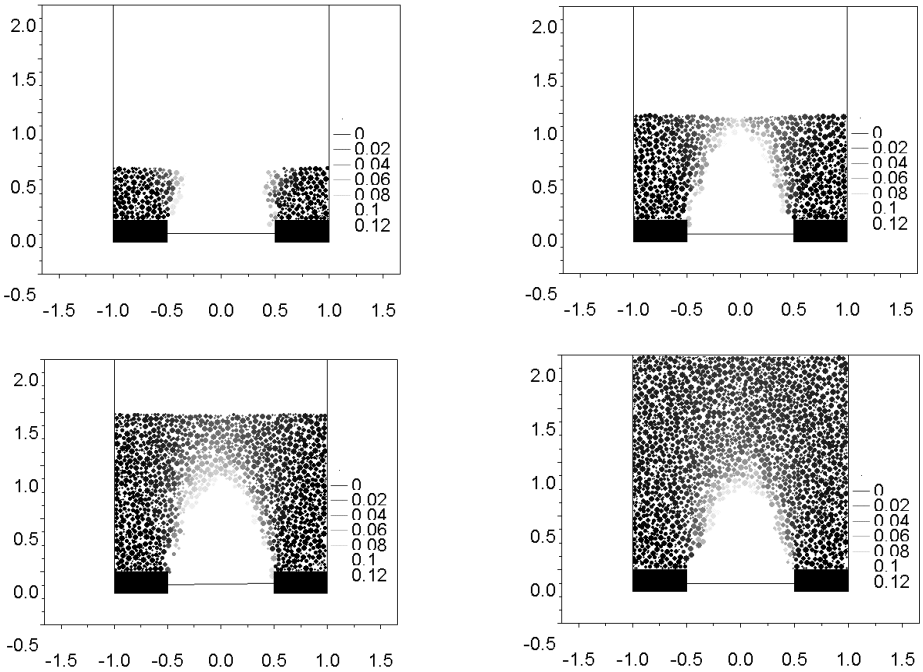


Fig. 12. Displacement field of the particles in a cross section of the granular layer ($M_3$) for $\delta = 0.12$ m and for different layer thicknesses (gray scale unit [m])

The graphic representation of the displacement of the particles in a cross section for $M_3$ is given in figure 12. The variation of surface settlements with $H$ is the same

for $M_3$ as for $M_1$ and $M_2$ (figure 13) but the settlement values are lower for $M_3$. Moreover, we can notice that the relative slipping of the part of the granular material above the mobile plate is reduced for $M_3$ (figure 14).

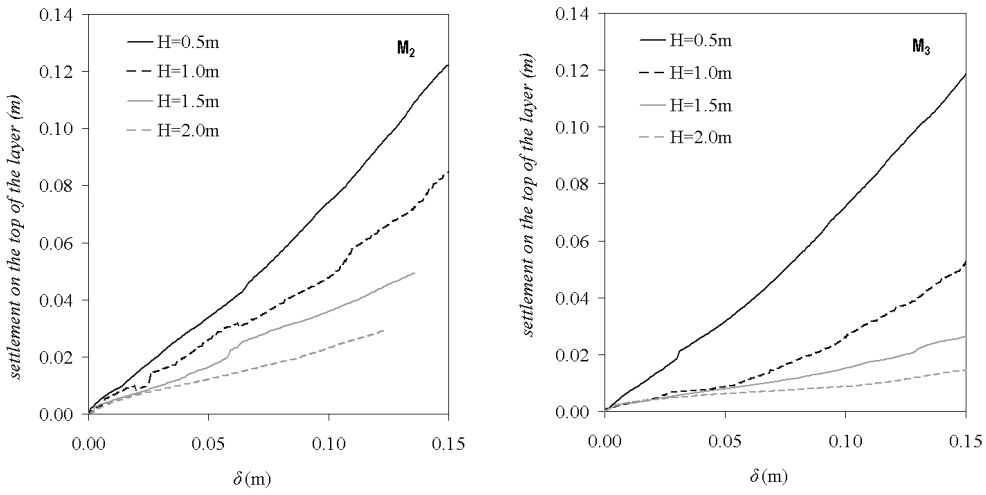


Fig. 13. Maximal values of the settlement measured on the surface of the granular layer for $M_2$ (left) and $M_3$ (right)

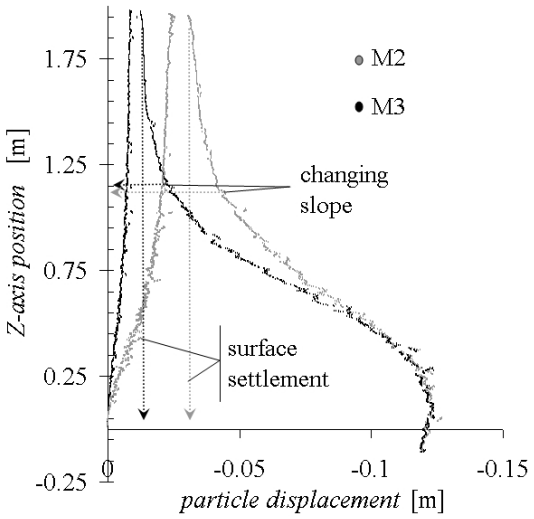


Fig. 14. Vertical displacements along (Δ) (left curves) and (Δ′) (right curves) for $M_2$ and $M_3$ ($\delta = 0.12$ m)

## 4. APPLICATION TO A PILED EMBANKMENT

The pattern modelled in this study represents a 1.0-m square mesh of a structure. Each support (0.2 m × 0.2 m) put in the corner of the mesh in figure 2 represents a quarter of a pile cap. The materials $M_1$, $M_2$ and $M_3$ have been tested in this application, the granular layer thickness $H$ varying between 0.5 m and 2.0 m. The behaviour of each material is assessed by an efficacy defined by:

$$E_P = \frac{W_P}{W_T}, \tag{6}$$

where $W_P$ is the vertical force exerted on the piles and $W_T$ stands for the total weight of the granular material involved. The values obtained by numerical modelling will be compared with these given by two analytical methods, taking into account the formation of hemispheric arches over a network of piles [2]–[4].

### 4.1. THE INLFUENCE OF THE PARTICLE SHAPE BY COMPARING $M_1$ AND $M_2$

The effect of $H$ on the effort $F$ measured at the bottom of a horizontal wall is totally different in the piled embankment configuration than that in the trap-door problem (figure 15). For $M_1$ and $M_2$, there is no convergence of the curves when $H$ increases. The critical height $H_{crit}$ is much more important than in the previous configuration and is not reached here: $H_c \geq 2.0$ m.

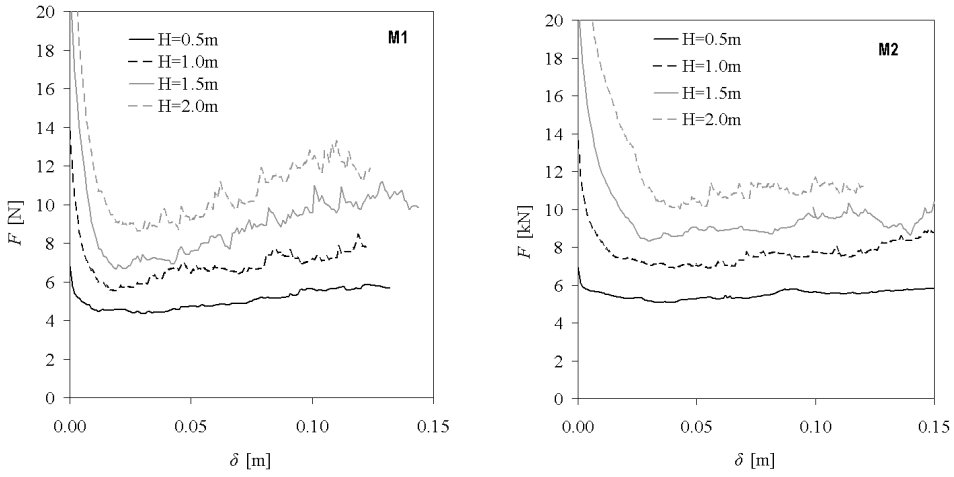


Fig. 15. $F$ versus $\delta$ in the piled embankment problem for $M_1$ (left) and $M_2$ (right)

As for the effect of shape, the minimal value of $F$ reached is lower in the case of $M_1$. Though, after this minimum is exceeded, the effort $F$ is quasi-constant for $M_2$, whereas it increases with $\delta$ for $M_1$. With regard to efficacies, the difference between $M_1$ and $M_2$ is less than 5% (figure 16). The macroscopic shear strength is an essential parameter of the load transfer intensity when applied in piled embankments.

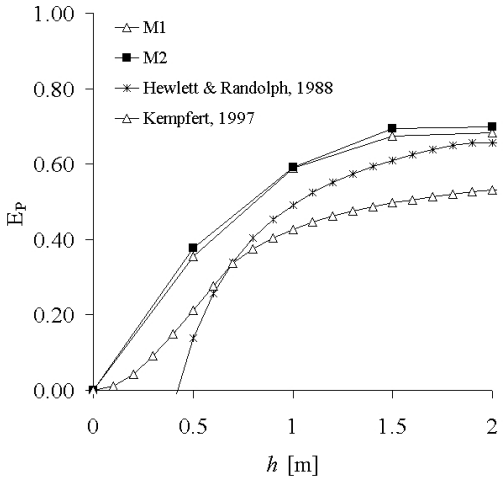


Fig. 16. Comparison of efficacies obtained from numerical results ($M_1$ and $M_2$) and from two design methods [2], [3]

We can notice a great difference in the effect of shape when applied to the trap--door. The critical thickness $h_c$ above which the effort $F$ is independent of $H$ is not reached for the geometry tested here. The shear strength necessary to observe this critical height is higher in the case of the piled embankment than for the trap-door.

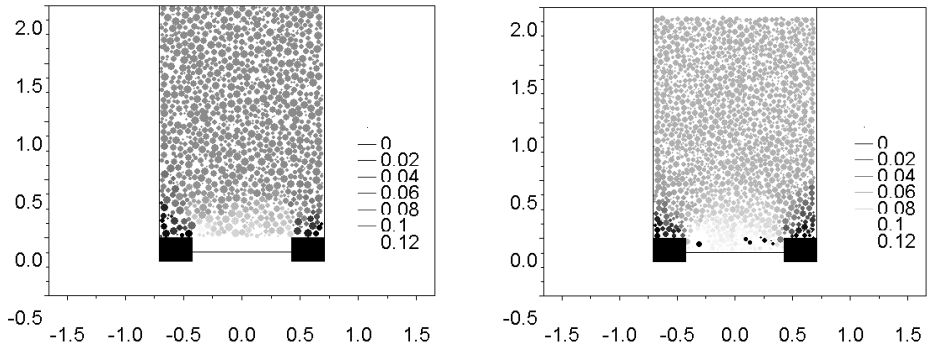


Fig. 17. Displacement fields of the particles in a vertical diagonal cross section of the granular layer for materials $M_1$ (left) and $M_2$ (right); $\delta = 0.12$ m and $H = 2.0$ m (gray scale unit [m])

The displacement fields in a cross section for the thickness $H$ = 2.0 m show that the kinematics of the granular layer over the network of piles differs fundamentally from that over a trench (figure 17). The upper part of the granular layer lays on fixed portion of granular material, located on each support.

This upper block moves as a unique solid (figure 18). In this case, we can find a limit of equal settlement, defined by the $Z$-axis position, in the layer above which the displacements of particles located in the same horizontal plane are equal. This means that the top of the layer remains horizontal and no surface differential settlements are observed.

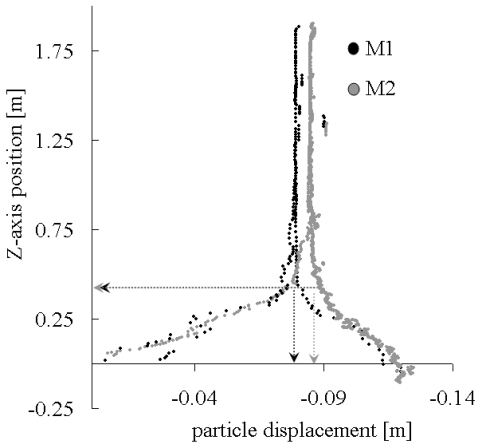


Fig. 18. Vertical displacements along (Δ) (left curves) and (Δ′) (right curves) for $M_2$ and $M_3$ ($\delta$ = 0.12 m)

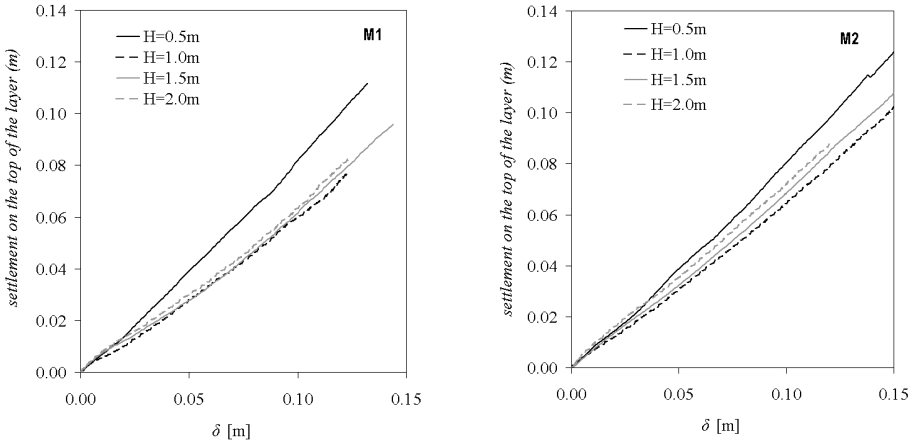


Fig. 19. Maximal values of the settlement measured on the surface of the granular layer for $M_1$ (left) and $M_2$ (right)

Contrary to the trap-door, the settlements do not vary for $H \geq 1.0$ m. However, the settlement are rather the same for $M_1$ and $M_2$.

### 4.2. INLFUENCE OF THE PEAK FRICTION ANGLE BY COMPARING $M_2$ AND $M_3$

The behaviour of $M_3$ in a configuration of a piled embankment is different from the behaviour of the two other materials (figure 20). Indeed, when $\delta$ increases, $F$ reaches a minimal value which is not dependent on $H$ anymore. The critical height $H_c$ above which the load transfer rate does not vary anymore is dependent on the shear strength (for $M_3$: $H_c \leq 0.5$ m).

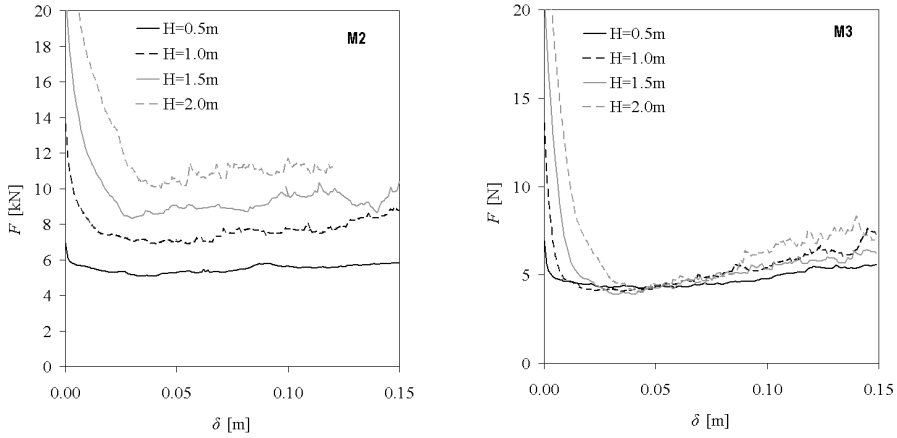


Fig. 20. $F$ versus $\delta$ in the piled embankment problem for $M_2$ (left) and for $M_3$ (right)

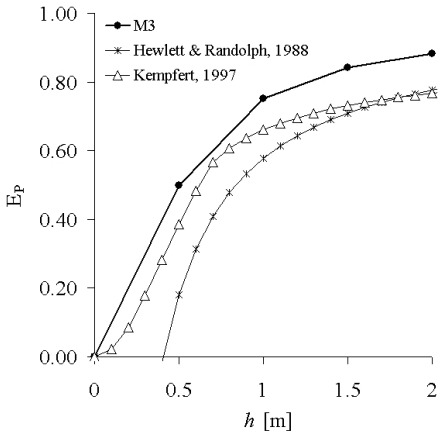


Fig. 21. Comparison of the efficacies obtained from numerical results ($M_3$) and from two design methods [2], [3]

Better shear strength properties involve higher efficacies. For $H$ = 2.0 m, 69% of the $M_1$ or $M_2$ granular material weight are transferred to the piles, while 89% are transferred with $M_3$ (figure 21). However, the comparison of the efficacies given by [2] and [3] with the numerical results leads to the same conclusions as previously: the analytical methods underestimate the efficacies.

As for the kinematics (figure 22), the mechanism involved with $M_3$ is the same as previously. The position of the equal settlement limit (0.75 m above pile top) is influenced neither by particle shape nor by $\varphi_{peak}$ (figure 23). However, the surface settlements are reduced (figure 24).

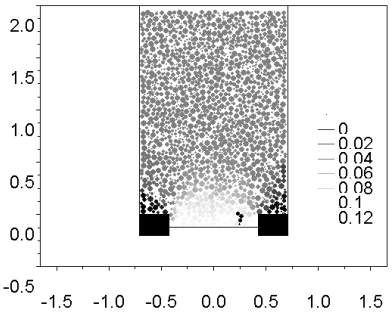


Fig. 22. Displacement field of the particles in a vertical diagonal cross section of the granular layer for materials $M_3$; $\delta$ = 0.12 m and $H$ = 2.0 m (gray scale unit [m])

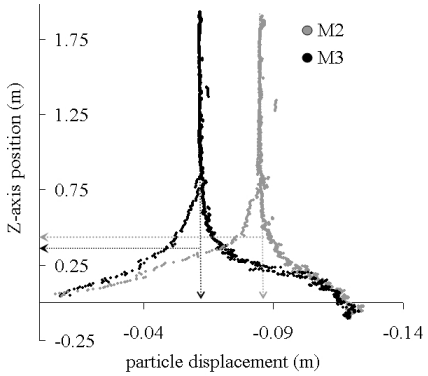


Fig. 23. Vertical displacements along (Δ) (left curves) and (Δ′)(right curves) for $M_2$ and $M_3$ ($\delta$ = 1.2 m)

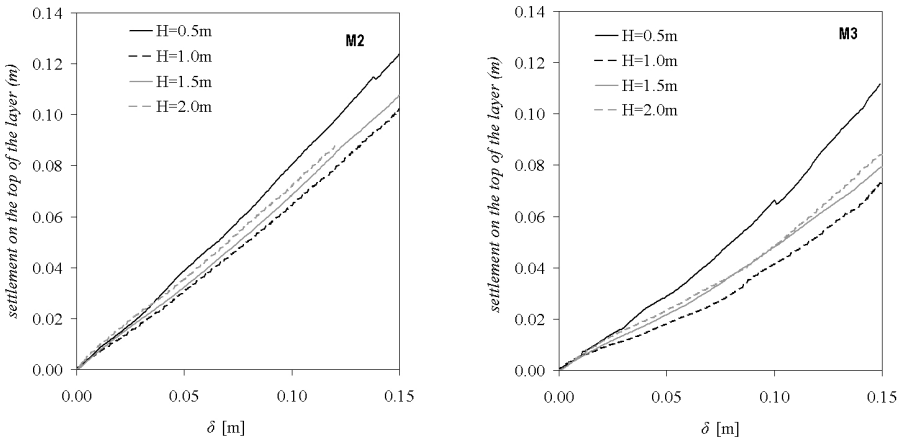


Fig. 24. Maximal values of the settlement measured on the surface of the granular layer for $M_2$ (left) and $M_3$ (right)

## 5. CONCLUSION

The results presented here lead to several major conclusions. The first one is that the load transfer intensity is directly related to the shear strength and not influenced by shape parameters. Kinematics is influenced by both shear strength and particle shape.

In the case of the trap-door problem, as in the description of Terzaghi, there is a relative slipping between the granular material above the trap-door and the remaining material. But the slipping is reduced for great values of layer thickness, in particular in its upper part. This is the reason for a divergence observed between numerical and analytical results.

In the case of a granular layer over a network of piles, a shear strength level can make the load transfer intensity independent of the layer thickness. In addition, differential settlements on the top of the layer can be reduced to zero for the reasonable layer thickness values.

The difference between the existing methods for the prediction of the load transfer intensity and the numerical results presented here shows the need to refine them. Indeed, the model of Terzaghi has the disadvantage that it, for example, does not take into account the arching effects that occur in the granular material which makes, in reality, the load transfer intensity much more important than that predicted. The calculation methods for piled embankments presented here take into account the forming of arches and so the difference is reduced. But the idealized arches considered lead to the underestimation of the load transfer again.

## REFERENCES

[1] TERZAGHI K., *Theoretical soil Mechanics*, New York, 1943, Wiley.

[2] HEWLETT W.J., RANDOLPH M.F., *Analysis of piled embankment*, Ground engineering, 1988, 21(3), 12–18.

[3] LOW B.K., TANG S.K., CHOA V., *Arching in piled embankments*, Journal of Geotechnical and Geoenvironmental Engineering, 1994, 120(11), 1917–1938.

[4] EBGEO, *Empfehlungen für Bewehrungen aus Geokunststoffen*, Deutsche Gesellschaft für Geotechnik (Hrsg.) Verlag Ernst & Sohn, Berlin, 1997, Germany.

[5] CUNDALL P.A., STRACK O.D.L., *A discrete numerical model for granular assemblies*, Géotechnique, 1979, 29(1), 47–65.

[6] DONZÉ F.V., MAGNIER S.-A., *Spherical Discrete Element Code*, [in:] *Discrete Element Project Report no. 2*. GEOTOP, Université du Québec à Montréal, 1997.

[7] CHAREYRE B., VILLARD P., *Dynamic spar elements and DEM in two dimensions for the modelling of soil-inclusion problems*, Journal of Engineering Mechanics – ASCE, 2005, 131(7), 689–698.

[8] COMBE G., ROUX J.-N., *Discrete numerical simulation, quasi-static deformation and the origin of strain in granular materials*, 3ème Symp. Int. sur le Comportement des sols et des roches tendres, Lyon, 22–24 Septembre 2003, [in:] Di Benedetto et al., 1071–1078.